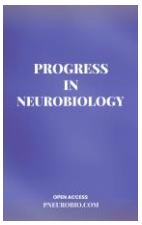

Progress in Neurobiology

Journal Homepage: pneurobio.com

Research Article

Serine-129 Phosphorylated α-Synuclein Regulates Endoplasmic Reticulum-Mitochondria Calcium Homeostasis via Interaction with VAPB and PTPIP51 in an α-Synuclein-induced Parkinson Disease Model

Weijin Liu[1, 2#], Jie Jiao[1#], Zihao Wang[1], Tie Wang[1], Ge Gao[1] and Hui Yang[1*]

[1]Department of Neurobiology, School of Basic Medical Sciences, Capital Medical University, Beijing Key Laboratory of Neural Regeneration and Repair, Beijing Key Laboratory on Parkinson's Disease, Key Laboratory for Neurodegenerative Disease of the Ministry of Education, Beijing Institute of Brain Disorders, Collaborative Innovation Center for Brain Disorders, Beijing, China

[2]China Rehabilitation Science Institute, China Rehabilitation Research Center, Beijing Key Laboratory of Neural Injury and Rehabilitation, and School of Rehabilitation Medicine, Capital Medical University, Beijing, China

#Contributed Equally

ARTICLE INFO

Article history:
Received: 3 August, 2023
Accepted: 30 August, 2023
Published: 13 September 2023

Keywords:
α-synuclein, phosphorylation, endoplasmic reticulum, mitochondria, calcium

ABSTRACT

Serine-129 phosphorylated α-synuclein (p-α-syn), accounting for nearly 90% of α-synuclein (α-syn) found in Lewy bodies (LBs), is linked to the pathogenesis of Parkinson's disease (PD). The molecular targets for the cytotoxic effect of p-α-syn are not fully understood; however, so we sought to determine the role of p-α-syn in cell injury and describe the underlying molecular mechanism. Mitochondrial dysfunction was observed in primary neurons from Thy1-SNCA transgenic mice. Using co-immunoprecipitation coupled with mass spectrometry, we screened the p-α-syn interacting proteins in the midbrains of TG mice and validated the interaction with vesicle-associated membrane protein-associated protein (VAPB) and protein tyrosine phosphatase interacting protein 51 (PTPIP51), which are both located in the mitochondrion-associated endoplasmic reticulum (ER) membrane. VAPB binds to PTPIP51 tethering ER and mitochondria and has an important role in the transport of calcium. We showed that inhibition of α-syn phosphorylation at ser 129 increased the interaction between VAPB and PTPIP51. Moreover, we also demonstrated that inhibition of α-syn phosphorylation at ser 129 alleviated ER and mitochondrial calcium overload. These findings suggest that p-α-syn is involved in regulation of the ER and mitochondrial calcium, which provides new insight into the mechanism by which p-α-syn induces cellular toxicity and neurodegeneration.

1. Introduction

Parkinson's disease (PD) is a progressive neurodegenerative disorder affecting individuals >65 year of age [1]. The main pathologic hallmarks of PD are the selective loss of dopaminergic neurons in the substantia nigra pars compacta and the presence of intraneuronal proteinaceous cytoplasmic inclusions named lewy bodies (LBs) in the surviving dopamine neurons [2]. The major constituent of LBs is alpha-synuclein (α-syn), which has an essential role in the onset and progression of PD [3]. It is noteworthy that under pathologic circumstances, α-syn is deposited in a hyperphosphorylated form at the ser 129 residue (p-α-syn). Indeed. the majority of α-syn found in LBs is phosphorylated at the ser 129 [4].

Previous studies indicated that α-syn translocates to mitochondria and causes mitochondrial damage [5], including oxidant stress and disruption of calcium homeostasis [6]. Furthermore, the mitochondrion-associated endoplasmic reticulum (ER) membrane (MAM), in close proximity between mitochondria and a subdomain of the ER, has a crucial role in regulation of calcium signaling [6] and has been reported to be involved in PD and other neurodegenerative diseases [7, 8]. In pathologic scenarios, α-syn affects organelle junctions in MAM, thereby interfering with normal transport mechanisms [9]. Extensive evidence has demonstrated that α-syn establishes a direct interaction with MAM to regulate various essential cellular processes [10, 11].

Correspondence to: Hui Yang, Department of Neurobiology, School of Basic Medical Sciences, Capital Medical University, Beijing Key Laboratory of Neural Regeneration and Repair, Beijing Key Laboratory on Parkinson's Disease, Key Laboratory for Neurodegenerative Disease of the Ministry of Education, Beijing Institute of Brain Disorders, Collaborative Innovation Center for Brain Disorders, Beijing, China; Tel: 861083950373; Fax: 861083950373; E-mail: huiyang@ccum.edu.cn

DOI: 10.60124/j.PNEURO.2023.20.02

Co-localization of pathologic p-α-syn with mitochondria has been observed in patients, cells, and animal models with PD, causing mitochondrial dysfunction and implying a connection between p-α-syn and mitochondrial dysfunction [12]. It is unclear, however, whether p-α-syn localizes to the MAM and the pathogenic role of p-α-syn in regulation of mitochondria and MAM function.

Vesicle-associated membrane protein-associated protein (VAPB) is a highly-conserved transmembrane protein on the ER that is expressed in yeast, fruit flies, and mammals, and has an important role in mediating the connection between the ER and other organelles [13, 14]. In 2015 scientists identified the deletion of a valine residue at position 25 in sporadic PD patients, suggesting that VAPB dysfunction may be related to the pathogenesis of PD, but the specific mechanism has not been established [15]. Protein tyrosine phosphatase interacting protein 51 (PTPIP51) is a protein located on the outer mitochondria membrane that binds to VAPB to form a tethering complex existing in the MAM [16, 17]. This complex tethers the two organelles and has an important role in calcium transport from the ER to the mitochondria [18, 19]. Previous studies have reported that α-syn interaction with VAPB reduces the interaction between VAPB-PTPIP51 in SH-SY5Y cells, thus affecting calcium transport in the MAM [20].

In the current study we observed mitochondrial dysfunction in primary cortical neurons from Thy1-SNCA transgenic (TG) mice. Then we sought to determine the molecular mechanism underlying p-α-syn provocation of mitochondrial damage. We used co-immunoprecipitation coupled with mass spectrometry (CO-IP/MS) to screen p-α-syn interacting proteins in the midbrains of TG mice and validated the interactions between p-α-syn, and PTPIP51 and VAPB. Furthermore, we also evaluated the regulatory effect of α-syn and p-α-syn on calcium in the ER and mitochondria.

2. Results

2.1. α-syn Overexpression Causes Mitochondrial Disorder

Our previous research showed that the V63A and N65A mutations in α-syn restore mitochondrial complex I function and Δψm in HEK293T and MN9D cells [21], suggesting that α-syn plays a role in mitochondrial dysfunction. To determine the effects of α-syn on mitochondrial function in TG mice, we isolated and cultured primary cortical neurons from wild-type (WT) and TG mice overexpressing human α-syn. Mitochondrial complex I activity is directly related to mitochondrial function, specifically mitochondrial toxicity. Our results indicated that overexpression of α-syn resulted in remarkable reductions in mitochondrial complex I activity (Figure 1A) and the ATP level (Figure 1B) in primary cortical neurons. Furthermore, α-syn was significantly overexpressed in the production of reactive oxygen species [ROS] (Figure 1C), which are byproducts of mitochondrial respiration and may cause more damage to various cell components. In addition, the mitochondrial membrane potential was also decreased (Figure 1D). These results suggested that α-syn is toxic to mitochondria, thus affecting mitochondrial function.

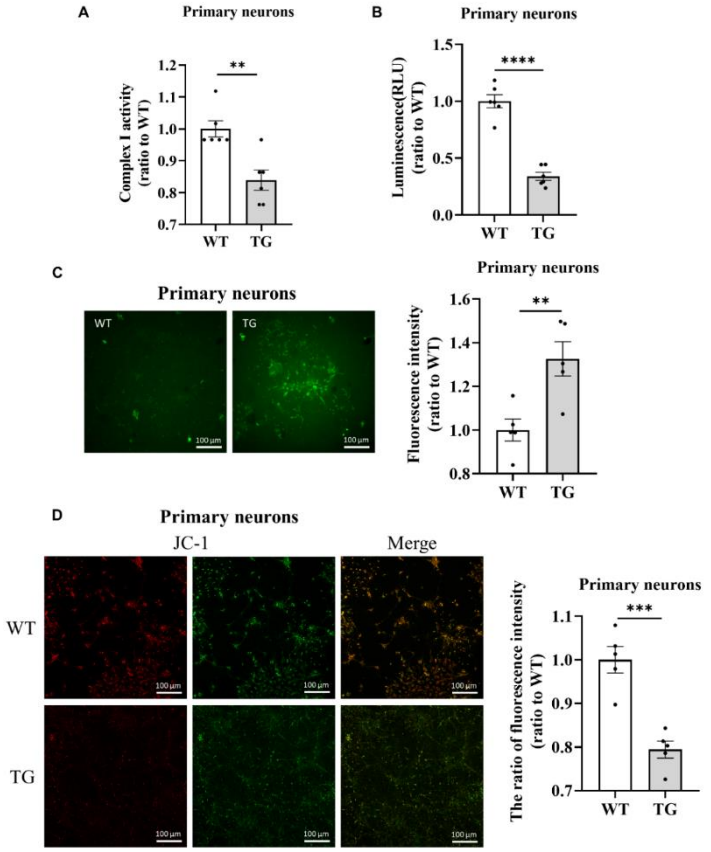

FIGURE 1: α-syn overexpression caused mitochondrial disorder in primary cortical neurons in WT and TG mice. **A)** Mitochondrial complex I activity was detected in primary neurons. **B)** ATP levels in primary neurons. **C)** The reactive oxygen species (ROS) level was examined using the ROS probe, DCFH-

DA, in primary neurons. Quantitative analysis of fluorescence intensity on the right. Scale bar, 100 μm. **D)** MMP was assessed using JC1 staining in primary neurons. Quantitative analysis of fluorescence intensity on the right. Scale bar, 100 μm. Data are expressed as the mean ± standard error of the mean (SEM; unpaired t-test). n: 4-6. ***P*<0.01, ***P＜0.001, ****P < 0.0001, vs. WT.

2.2. Identifying Proteins Interacting with p-α-syn and h-α-syn by CO-IP/MS

When α-syn is overexpressed, the intracellular level of p-α-syn is also elevated [22]. However, the specific role of p-α-syn in the pathogenesis of α-syn and underlying molecular mechanism remain unclear. The injurious effects of α-syn and p-α-syn on mitochondria prompted us to elucidate the underlying molecular mechanisms. Therefore, we performed CO-IP/MS to identify proteins that interact with α-syn and p-α-syn.

To ensure the accuracy of antigen enrichment by antibodies in the CO-IP assay, we tested the specificity of p-α-syn and h-α-syn antibodies and identified specific D1R1R and MJFR1 antibodies for use in CO-IP/MS experiments (Figure S1). As the flow diagram in (Figure 2A) shows, we performed a CO-IP assay using the midbrains of 13-month old TG mice. SDS-PAGE and silver staining results indicated successful enrichment of D1R1R and MJFR1 antibodies in p-α-syn and h-α-syn proteins (17 k Da), and the proteins interacting with p-α-syn and h-α-syn and were different (Figure 2B).

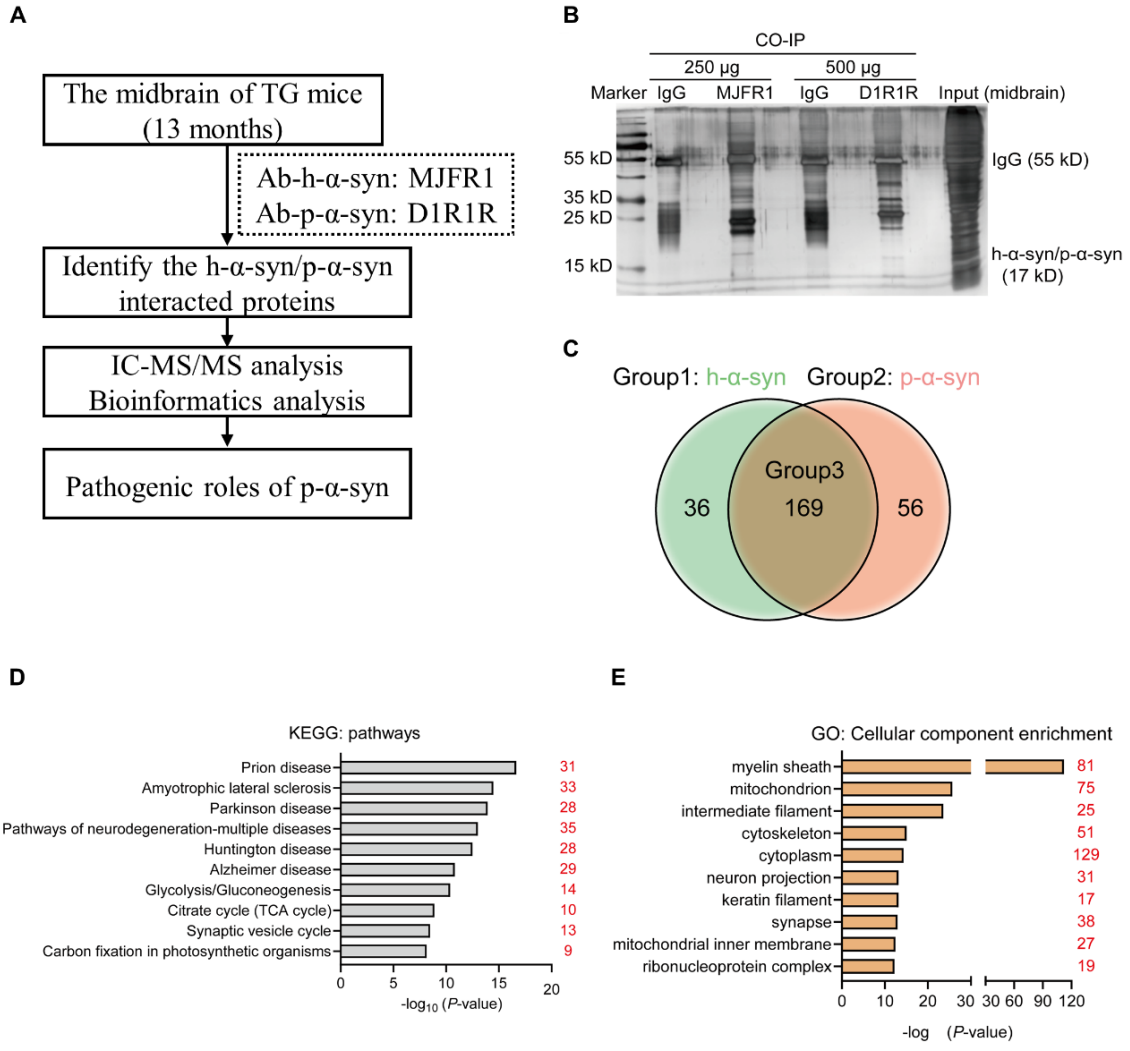

FIGURE 2: CO-IP/MS assays and the analysis of proteins interacting with p-α-syn. **A)** Flow diagram of CO-IP using D1R1R and MJFR1 antibodies and LC-MS/MS for the identification of p-α-syn and h-α-syn interacting proteins from the midbrains of 13-month old TG mice. **B)** SDS-PAGE and silver staining were used to detect the enrichment of h-α-syn, p-α-syn, and interacting proteins. IgG served as a control. **C)** Venn diagrams of interacting proteins. Group 1 (green), 36 proteins specifically interacted with h-α-syn. Group 2 (pink), 56 proteins specifically interacted with p-α-syn. Group 3 (brown), 169 proteins interacted with both h-α-syn and p-α-syn. (D, E).
D) KEGG analysis and **E)** GO-cellular component (GO-CC) analysis for 225 proteins interacted with p-α-syn. The red numbers indicate the number of interacting proteins contained in each term.

We searched the CO-IP/MS database and screened proteins which identified at least 2 peptides with ≥95% confidence (peptides 95%≥2). The venn diagram showed that 36 proteins (group_1) interacted with h-α-syn, 56 proteins (group_2) interacted with p-α-syn, and 159 proteins (group_3) interacted with p-α-syn and h-α-syn at the same time (Figure 2C). We further used the DAVID Bioinformatics Resources (2021 Update) website to determine the properties and biology of p-α-syn interacting proteins by kyoto encyclopedia of genes and genomes (KEGG) and gene ontology (GO) enrichment analysis.

The top 10 pathways identified by KEGG analysis ranked by p-values were as follows: prion disease; amyotrophic lateral sclerosis; PD; pathways of neurodegeneration-multiple diseases; huntington disease; alzheimer disease; glycolysis/gluconeogenesis; citrate cycle; synaptic vesicle cycle; and carbon fixation in photosynthetic organism in photosynthetic organisms (Figure 2D). The top 10 cellular component (CC) GO enrichment analysis ranked by p-values were as follows: myelin sheath; mitochondrion; intermediate filament; cytoskeleton; cytoplasm; neuron projection; keratin filament; synapse; mitochondrial inner membrane; and ribonucleoprotein complex (Figure 2E).

2.3. Subcellular Localization of p-α-syn in the Midbrains of TG Mice

Based on bioinformatics analysis, we have a macro understanding of subcellular localization of p-α-syn interacting proteins. For further validation, electron microscopy with immunogold labeling of p-α-syn was performed. In accordance with previous findings, the p-α-syn was specifically deposited in the cytoskeleton, nucleus, cytoplasm, synapses, mitochondria, ER, and MAM (Figures 3A-3G). The results are consistent with the CC-GO analysis above, suggesting that p-α-syn is closely related to the cytoskeleton, nucleus, cytoplasm, synapse, mitochondria, ER, and MAM.

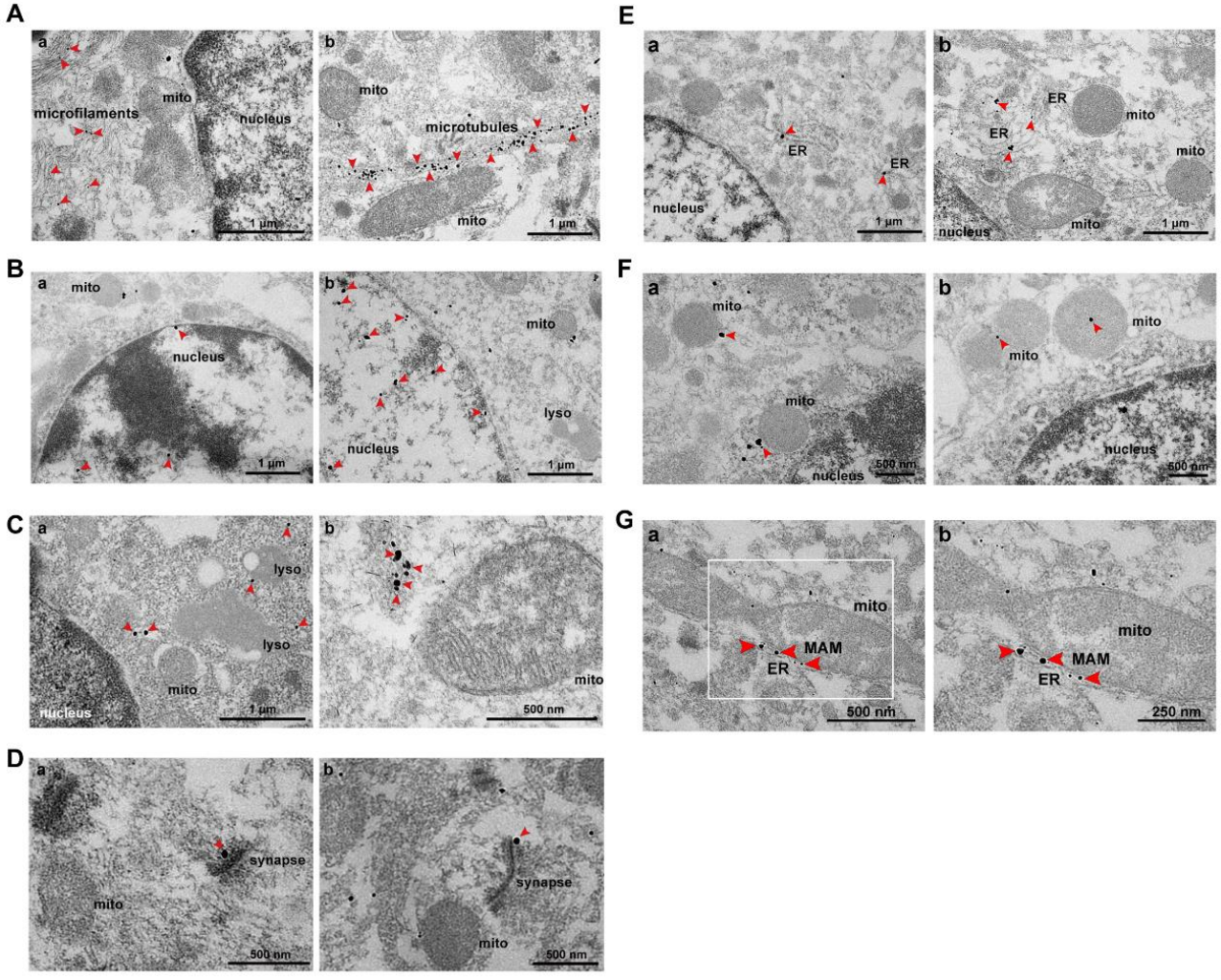

FIGURE 3: Electron microscopy with immunogold labeling of p-α-syn in the midbrains of TG mice. **A-G)** The p-α-syn was specifically deposited in the **A)** cytoskeleton, **B)** nucleus, **C)** cytoplasm, **D)** synapses, **E)** mitochondria, **F)** endoplasmic reticulum, and the **G)** MAM. The red arrow indicates the concentrated area of p-α-syn. White square, the area shown in higher magnification. Scale bar, 1 μm, 500 nm necrotic area of lymphocytes.

2.4. VAPB and PTPIP51 are Expressed in Midbrains of TG Mice and co-localized with p-α-syn.

P-α-syn is known to increase to 90% in LBs, suggesting that p-α-syn is associated with the disease state and has negative effects on neuronal functioning [23]. Because p-α-syn is in abundance under disease conditions, we were curious about the molecular mechanism underlying p-α-syn on cell functions.

Among p-α-syn interacting proteins distinguished from h-α-syn identified by CO-IP/MS, PTPIP51 ranked first and the seventh was VAPB. We determined the expression and distribution of VAPB and PTPIP51 using western blot and immunofluorescence. The western blot results showed that VAPB (Figure 4A) and PTPIP51 (Figure 4B) were expressed in RIPA and 2% SDS soluble fractions in the midbrains of mice, and the expression was unchanged in TG mice compared with α-syn knockout (KO) and WT mice. Immunofluorescence analyses showed that VAPB (Figure 4C) and PTPIP51 (Figure 4D) were expressed ubiquitously in cells and co-localized with p-α-syn, which was consistent with CO-IP/MS results.

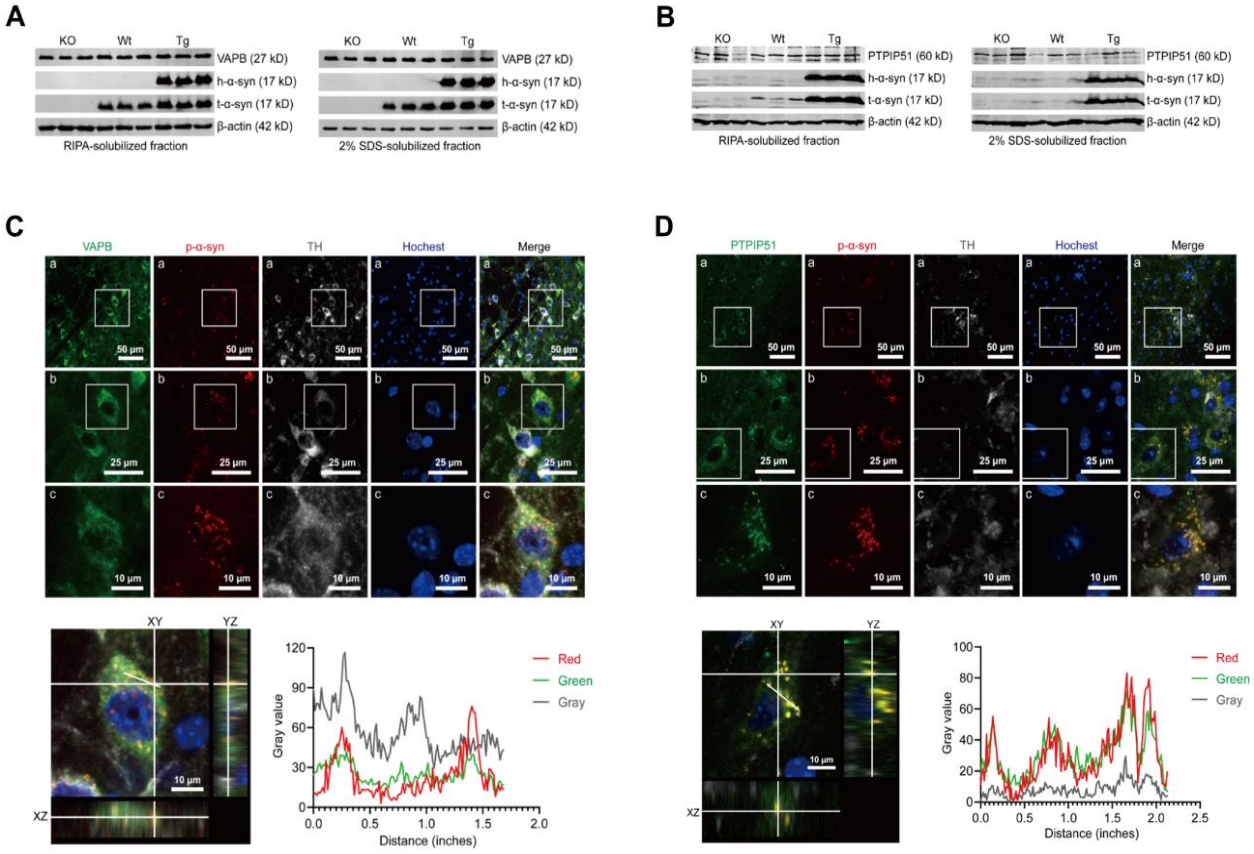

FIGURE 4: Expression and distribution of VAPB and PTPIP51 in midbrains of TG mice. **A)** VAPB and **B)** PTPIP51 expression in the midbrains of α-syn knockout (KO), WT, and TG mice by western blot. Left, RIPA soluble fractions. Right, 2% SDS soluble fractions. β-actin serves as the loading control. **C)** VAPB and **D)** PTPIP51 expression in the midbrains of TG mice by immunofluorescence. VAPB or PTPIP51(green), p-α-syn (red), dopaminergic neuron marker (tyrosine hydroxylase), TH (gray), and nuclei (blue). a-b, low magnification images; c, high magnification overlay images. White square, the area shown in higher magnification. Scale bar, **a)** 50 μm, **b)** 25 μm, **c)** 10 μm. Bottom left, orthogonal view shows co-localization of p-α-syn. Scale bar, 10 μm. Bottom right, co-localization was analyzed using ImageJ software.

2.5. Phosphorylation at Serine 129 is Necessary for the p-α-syn Interaction with VAPB

To verify the p-α-syn interaction with VAPB, we performed CO-IP analysis. VAPB interacted with p-α-syn (Figure 5A), but not h-α-syn (Figure 5B) in the midbrains of 13-month old TG mice. To further determine the necessity of phosphorylation at serine 129 in the interaction between α-syn and VAPB, SH-SY5Y cells were co-transfected with myc, myc-α-syn, or myc-α-syn S129A and VAPB-Flag-6 X His plasmids. P-α-syn, h-α-syn, h-α-syn S129A, and VAPB proteins were assessed by western blot and demonstrated that α-syn overexpression had no effect on the VAPB level (Figures S2 A and S2 B). CO-IP was performed using anti-Flag antibody after co-transfection of VAPB-Flag-6 X His with either myc-α-syn or myc-α-syn S129A plasmid in SH-SY5Y cells. There was an interaction between p-α-syn and VAPB (Figure 5C), but VAPB also partially interacted with h-α-syn, which is not phosphorylated at ser 129.

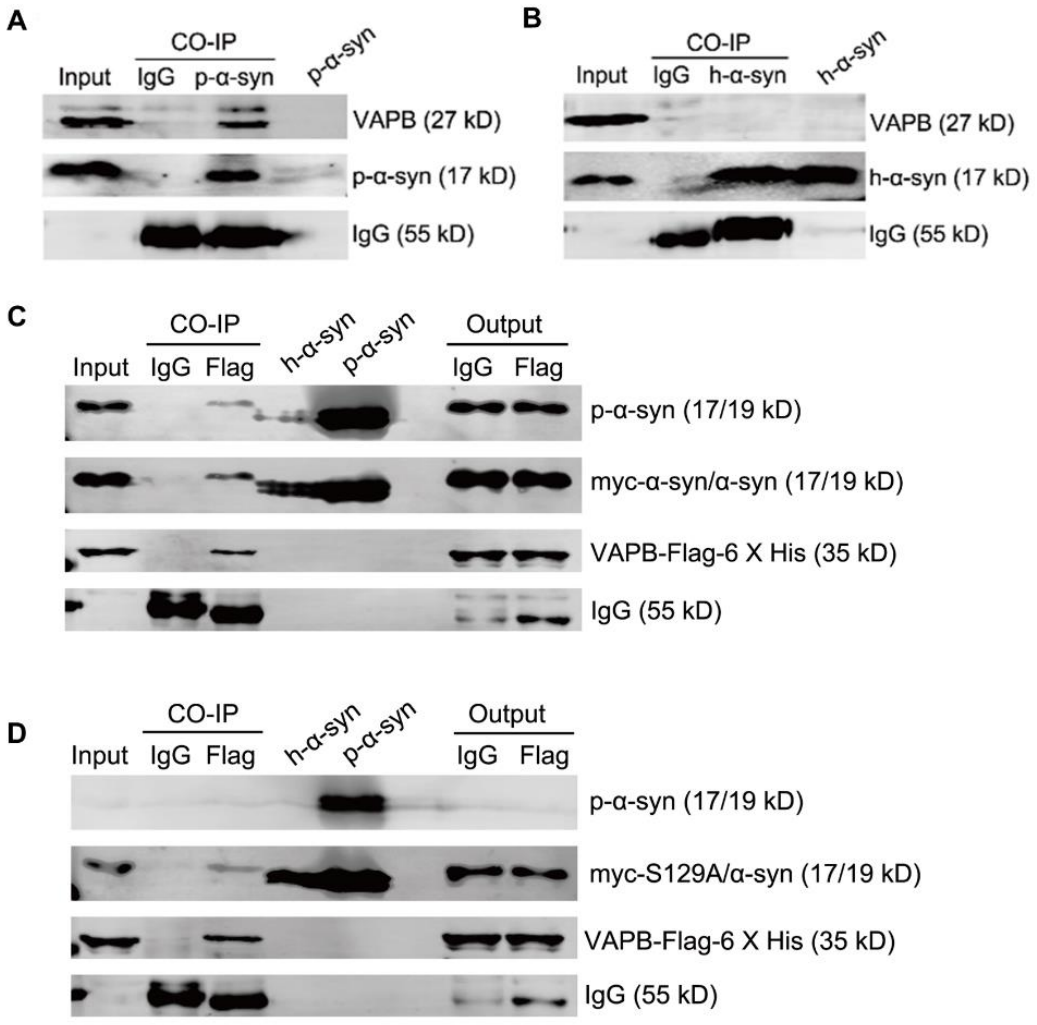

FIGURE 5: p-α-syn interacted with VAPB and phosphorylation at serine 129 promoted the interaction. (A, B) Interaction of p-α-syn, h-α-syn, and VAPB detected by CO-IP with antibodies against **A)** p-α-syn and **B)** h-α-syn in the midbrains of 13-month old TG mice. IgG served as a control. **C)** SH-SY5Y cells were co-transfected with VAPB-Flag-6 X His and myc-α-syn plasmids. CO-IP was performed using flag antibody to verify the interaction between h-α-syn, p-α-syn, and VAPB. **D)** SH-SY5Y cells were co-transfected with VAPB-Flag-6 X His and myc-α-syn S129A plasmids. CO-IP was performed using flag antibody to verify the interaction between h-α-syn and VAPB. Purified h-α-syn and p-α-syn proteins (200ng) were used as positive controls.

2.6. Phosphorylation at Serine 129 is Essential for the p-α-syn Interaction with PTPIP51

Having verified that p-α-syn interacts with VAPB, we further validated the interaction between p-α-syn and PTPIP51. SH-SY5Y cells were co-transfected with myc-α-syn and PTPIP51-Flag-6 X his plasmids. CO-IP assay using MJFR1 and D1R1R antibodies revealed that there was interaction between p-α-syn and VAPB, and p-α-syn and PTPIP51 (Figure 6A); however, we did not detect an interaction between h-α-syn, and VAPB and PTPIP51 (Figure 6B).

To further investigate the necessity of phosphorylation at serine 129 in the interaction between α-syn and PTPIP51, we performed reverse CO-IP using flag antibody. We first examined protein expression after transfection. SH-SY5Y cells were co-transfected with myc, myc-α-syn, or myc-α-syn S129A and PTPIP51-Flag-6 X his plasmids. Western blot results indicated that the h-α-syn, h-α-syn S129A, p-α-syn, and PTPIP51 proteins were successfully expressed and the level of PTPIP51 protein was not affected by overexpression of α-syn (Supplementary Figures 2C and 2C). We then performed CO-IP using anti-Flag antibody after co-transfection of VAPB-Flag-6 X his with myc-α-syn or myc-α-syn S129A plasmid in SH-SY5Y cells. There was an interaction between p-α-syn and PTPIP51 (Figure 6C), but no interaction was detected between PTPIP51 and hα-syn, which is not phosphorylated at ser 129 (Figure 6C).

Taken together and based on the above CO-IP results in TG mouse midbrain tissues and SH-SY5Y cells, we showed that phosphorylation at ser 129 is critical for the interactions between h-α-syn, and VAPB and PTPIP51. Because phosphorylation at ser 129 in α-syn is associated with PD pathogenesis, phosphorylation at ser 129 in α-syn may regulate VAPB and PTPIP51 protein function by affecting the interactions between h-α-syn, and VAPB and PTPIP51.

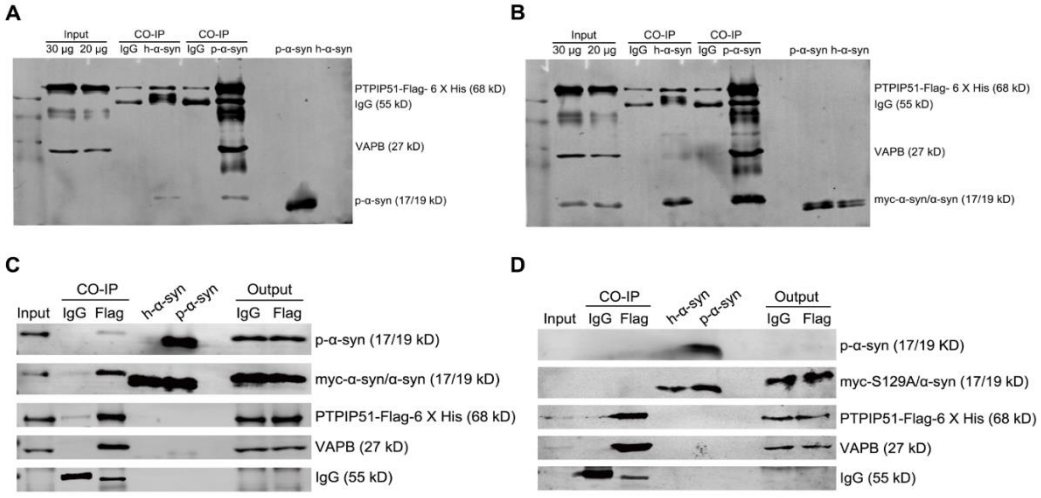

FIGURE 6: p-α-syn interacted with PTPIP51, unlike h-α-syn. (A, B) SH-SY5Y cells were co-transfected with myc-α-syn and PTPIP51-Flag-6 X His plasmids. Interaction of h-α-syn, p-α-syn, and PTPIP51 detected by CO-IP using **A)** p-α-syn and **B)** h-α-syn antibodies in SH-SY5Y cells. IgG served as a control. (C, D) SH-SY5Y cells were co-transfected with myc-α-syn and **C)** PTPIP51-Flag-6 X His, myc-α-syn S129A, and **D)** PTPIP51-Flag-6 X His plasmids. CO-IP was performed using flag antibody to verify the interaction between p-α-syn, h-α-syn, and VAPB. Purified p-α-syn and h-α-syn proteins (200 ng) were used as positive controls.

2.6. Inhibition of α-syn Phosphorylation at Ser 129 Tended to an Increase Interaction between VAPB and PTPIP51 in SH-SY5Y Cells

The interaction between the integral ER protein, VAPB, and outer mitochondrial membrane protein, PTPIP51, is one of the best characterized tethers in the MAM. Specifically, the interaction between VAPB and PTPIP51 regulates calcium exchange between the two organelles. It has been reported that α-syn weakens the interaction between VAPB and PTPIP51 in the MAM by interacting with VAPB, which in turn impairs calcium transport in the ER and mitochondria. To determine whether α-syn phosphorylation at ser 129 also affects the interaction of VAPB with PTPIP51, we performed the CO-IP assay in SH-SY5Y cells which were transfected with myc, myc-α-syn, or myc-α-syn S129A. Given the low endogenous PTPIP51 expression in SH-SY5Y cells, we co-transfected PTPIP51-Flag-6 X his plasmids. Western blot confirmed that p-α-syn, h-α-syn, and PTPIP51 were successfully expressed (Figures 7A and 7B). CO-IP results demonstrated that α-syn overexpression did not significantly affect the interaction between VAPB and PTPIP51, but inhibition of α-syn phosphorylation at ser 129 tended to an increase interaction between VAPB and PTPIP51 (Figures 7C and 7D).

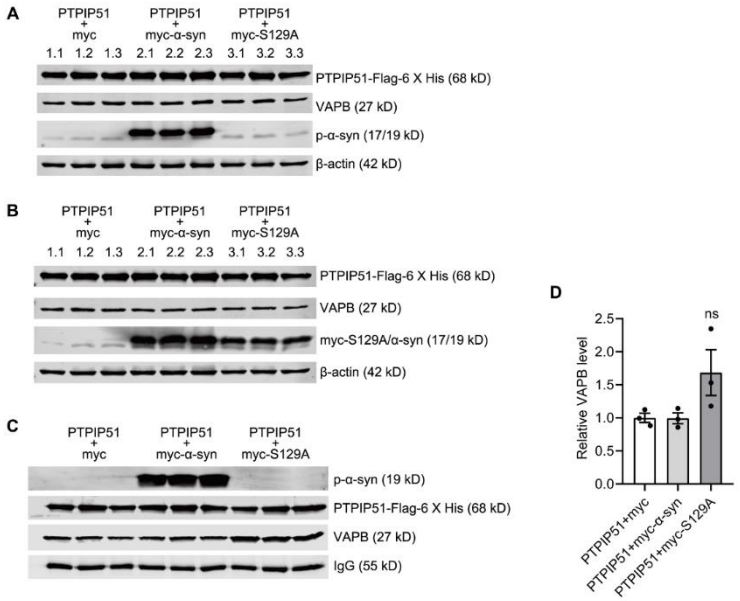

FIGURE 7: α-syn phosphorylation at ser 129 affected the interaction between VAPB and PTPIP51. SH-SY5Y cells were co-transfected with myc, myc-α-syn, myc-α-syn S129A, and PTPIP51-Flag-6 X His plasmids. (A, B) P-α-syn, h-α-syn, VAPB, and PTPIP51 were expressed by Western blot using antibodies specific to **A)** p-α-syn and **B)** h-α-syn. β-actin serves as the loading control. **C)** Flag antibody was used for the CO-IP assay to enrich PTPIP51 in cell

components. The protein levels of p-α-syn, VAPB, and PTPIP51 were detected by western bolt. **D)** Quantitative analysis of the VAPB level in (C). The results are expressed as the mean ± standard error of the mean (SEM; One-way ANOVA with Tukey's multiple comparisons test, n=3). ns: no significance.

2.7. Inhibition of α-syn Phosphorylation at Ser 129 Alleviated ER and Mitochondrial Calcium Overload in SH-SY5Y Cells

VAPB interacts with PTPIP51 to modulate calcium delivery at ER-mitochondria contact sites. We therefore determined whether α-syn phosphorylation at ser 129 affected the calcium equilibrium in the ER and mitochondria. We first examined the effect of α-syn overexpression and phosphorylation at ser 129 on ER calcium variation. SH-SY5Y cells were co-transfected with myc, myc-α-syn, or myc-α-syn S129A plasmids, and the ER calcium level was determined by the ER calcium-specific fluorescent probe (Mag-Fluo-AM) 30 h post-transfection. The ER calcium concentration of α-syn overexpression tended to increase compared with the myc control, and inhibition of phosphorylation at ser 129 reduced the calcium overload due to α-syn overexpression (Figures 8A & 8B). The cell count showed that inhibition of phosphorylation at ser 129 alleviated cytotoxicity caused by α-syn (Figure 8C).

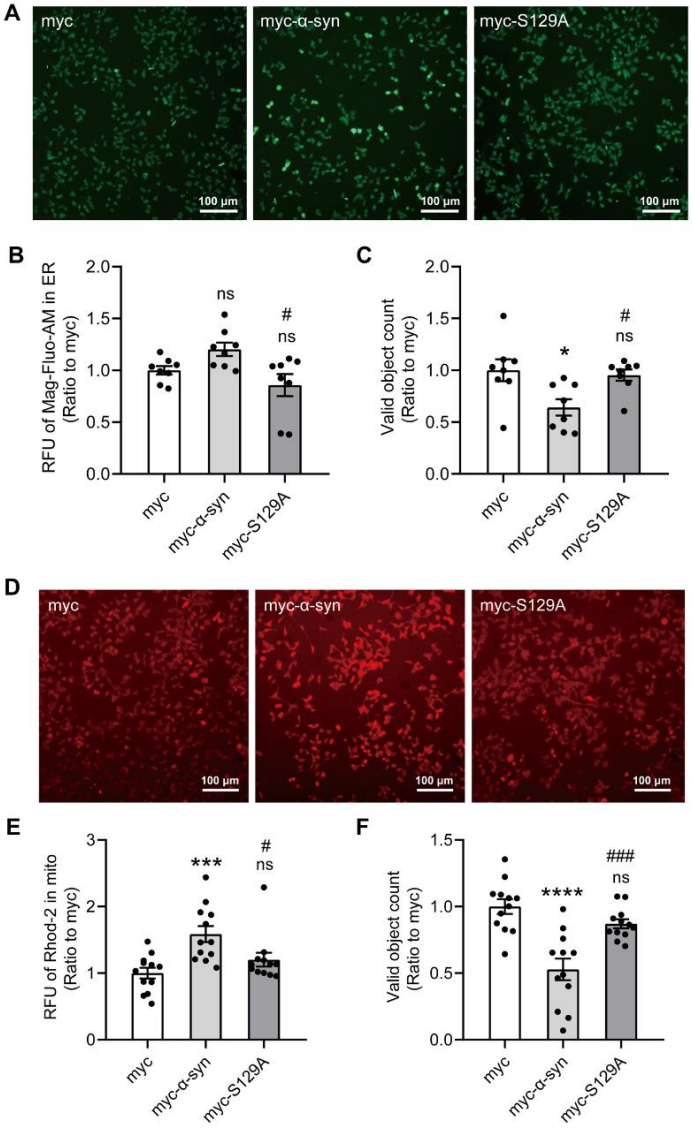

FIGURE 8: Inhibition of α-syn phosphorylation at ser 129 alleviated ER and mitochondrial calcium overload. SH-SY5Y cells were co-transfected with myc, myc-α-syn, and myc-α-syn S129A plasmids and the calcium concentration was measured 30 h after transfection. **A)** The ER calcium concentration was determined using Mag-Fluo-AM, the probe specific for ER calcium. Green fluorescence intensity reflects the concentration of calcium. Scalebar, 100μm. **B, C)** Statistical analysis of green fluorescence intensity (C) and **D)** numbers of SH-SY5Y cells. **E)** The mitochondria calcium concentration was determined using Rhod-2-AM, the probe specific for intra-mitochondrial calcium. Red fluorescence intensity reflects the concentration of calcium. Scalebar, 100μm. **F, G)** Statistical analysis of red fluorescence intensity (F) and **G)** numbers of SH-SY5Y cells. Data are expressed as the mean ± standard error of the mean (SEM; One-way ANOVA with Tukey's multiple comparisons test). n = 8, 12; ****P < 0.0001, ***P < 0.001, *P < 0.05 vs. myc, ###P < 0.001, #P < 0.05 vs. myc-α-syn; ns, no significance.

We further examined the effects of α-syn overexpression and phosphorylation at ser 129 on mitochondrial calcium. Similarly, SH-SY5Y cells were co-transfected with myc, myc-α-syn, or myc-α-syn S129A plasmids, and the levels of mitochondrial calcium were detected by the mitochondrial calcium-specific fluorescent probe (Rhod-2-AM) 30 h post-transfections. The mitochondrial calcium concentration of the myc-α-syn overexpression group was significantly increased, and inhibition of phosphorylation at ser129 alleviated the mitochondrial calcium overload caused by α-syn overexpression (Figures 8D & 8E). The cell count also showed that inhibition of phosphorylation at ser 129 alleviated cytotoxicity caused by α-syn (Figure 8F).

These results suggested that h-α-syn and h-α-syn phosphorylation at ser 129 are involved in the regulation of ER and mitochondrial calcium.

3. Discussion

P-α-syn is known to play a crucial role in the development of PD, but the exact molecular mechanism remains obscure. The current study showed that p-α-syn located in MAM and interacted with VAPB and PTPIP51 in α-syn-induced PD model. Phosphorylation at serine 129 is necessary for the interaction. P-α-syn also affected VAPB-PTPIP51 interaction and thus perturbed ER-mitochondria calcium homeostasis (Figure 9).

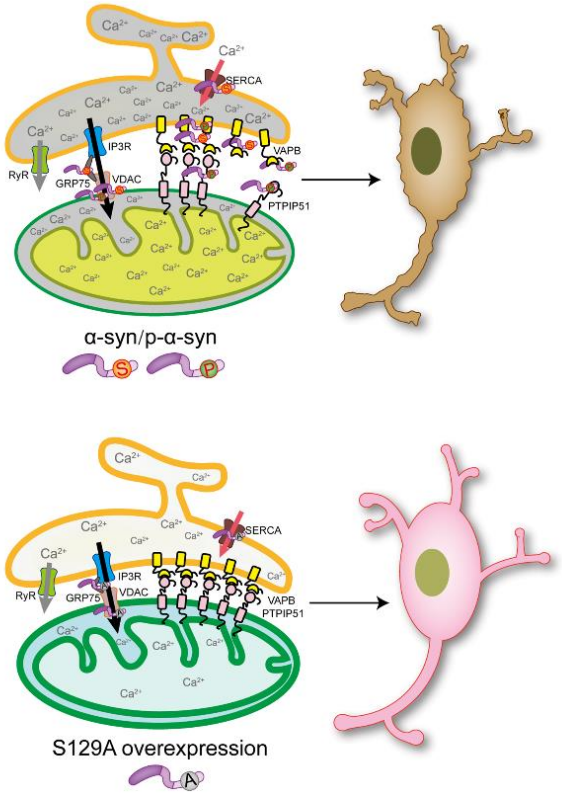

FIGURE 9: Phosphorylation at serine 129 partly influenced protein-protein interactions of α-syn in the midbrains of TG mice. The phosphorylation at serine 129 on α-syn was necessary for the interactions with VAPB and PTPIP51 and inhibition of phosphorylation at serine 129 partly alleviated calcium overload in the mitochondria and ER, and cell death caused by α-syn overexpression.

Even though the pathogenic mechanism underlying PD have not been established, toxic protein aggregation and mitochondrial dysfunction have been identified as key factors [24, 25]. The aggregation and accumulation of α-syn, a principal component of LBs and lewy neurites (LNs), which are characteristic PD pathologic findings, are closely related to the degenerative process [26].

It has been reported that α-syn enters the mitochondria, resulting in decreased mitochondrial membrane potential and respiratory chain damage. Notably, overexpression of α-syn has been shown to impede the trafficking of calcium within the ER and mitochondria [27]. Our group has also been studying mitochondrial dysfunction in PD. Our previous study showed that overexpression of α-syn caused an overload of mitochondrial calcium, which leads to opening of the permeability transition pore (mPTP) [21]. In this study we demonstrated that overexpression of α-syn in primary neurons caused mitochondrial damage including mitochondrial complex I activity, the ATP level, and MMP decreased, and the production of ROS increased (Figure 1).

Various post-translational modifications (PTMs) of α-syn exist in cells and phosphorylation at ser 129 appears to be the major PTM. Some studies have demonstrated that p-α-syn functions in structure, aggregation, cytotoxicity, and cell-to-cell transmission of pathogenic α-syn aggregates [28, 29]. Combining 2D western blot analysis and MS detection, it has been reported that p-α-syn increases abnormally among the total α-syn in the brain tissues of PD patients [4, 26, 30]. In a recent study, Moors TE observed the distribution of p-α-syn in mature LBs three-dimensional structures using super-resolution microscopy [31]. LBs were shown to be distributed in an onion-skin pattern from the inside out. The N-terminal and NAC region of α-syn are located in the

core region, and C-terminal phosphorylation at ser 129 are located in the LB outer layer. It was further confirmed that p-α-syn has an important role in the formation of LBs. To better understand the cause of this abnormal p-α-syn increase and the pathogenesis of PD in which p-α-syn is involved, we attempted to determine the molecular mechanism underlying the disease.

We detected and identified the differential proteins interacting with h-α-syn and p-α-syn by CO-IP assay using MJFR1 and D1R1R antibodies and further MS analysis in the midbrains of a 13-month old parkinsonian mouse model using TG mice. There were 169 proteins interacting with p-α-syn and h-α-syn; 36 proteins interacted specifically with h-α-syn and 56 proteins interacted specifically with p-α-syn. These differential proteins may be involved in the pathogenic mechanism underlying p-α-syn. In contrast to a proteomics analysis, which reported that non-phosphorylated α-syn short peptides enriched more mitochondria-related proteins than phosphorylated short peptides [32], the present study demonstrated that proteins that interact with p-α-syn ware widely distributed in the myelin sheath, mitochondria, intermediate filaments, cytoskeleton, and cytoplasm. The wide distribution of p-α-syn was later verified by immunogold electron microscopy (Figure 3). We preliminarily considered this finding was due to differences in protein enrichment methods, sample sources, and MS methods. These proteins are also involved in a variety of diseases, of which PD ranks third. The GO and KEGG bioinformatic analysis provided objective and clear data for us to better understand the biological processes involved in p-α-syn (Figure 2).

Based on the above CO-IP/MS results, we identified two interesting differential proteins (VAPB and PTPIP51), which were localized at the MAM. The interactions of VAPB and PTPIP51 with α-syn depended on phosphorylation at ser 129. Recently, damage of ER-mitochondria signaling has been observed in PD and other neurodegenerative diseases, leading to a disruption of vital processes including dysregulation of calcium signaling, autophagy, ATP production, and ER stress responses, thus causing eventual neurodegeneration [33-36]. ER-mitochondria signaling requires close physical contact between the two organelles (the MAM) and involves many tethering proteins that are used to recruit regions of the ER to the mitochondria. One of the tethering proteins involves an interaction between VAPB and PTPIP51 [37]; however, the relationship between p-α-syn and VAPB and PTPIP51 has not been reported.

In this study we showed that p-α-syn interacted specifically with VAPB and PTPIP51 in the midbrains of TG mice based on immunofluorescence and CO-IP experiments, indicating the interaction with α-syn depended on phosphorylation at ser 129 (Figures 4-6). Interestingly, inhibition of phosphorylation at ser 129 tended to increase the interaction between VAPB and PTPIP51 in SH-SY5Y cells (Figure 7). Thus, we speculate that p-α-syn perturbs ER-mitochondria associations by disrupting the VAPB and PTPIP51 interaction.

The VAPB-PTPIP51 tethers are known to be involved in many vital physiologic processes including inositol 1,4,5-trisphosphate (IP3) receptor-mediated calcium delivery from the ER to the mitochondria [19]. Subsequent functional experiments involving SH-SY5Y cells showed that phosphorylation at ser 129 was involved in calcium regulation in the mitochondria and ER, and inhibition of phosphorylation at ser 129 alleviated calcium overload in the mitochondria and ER caused by α-syn overexpression (Figure 8). Whether α-syn and phosphorylation at ser 129 affected the transport of calcium from the ER to mitochondria in MAM, however, needs to be verified by subsequent experiments.

In conclusion, our findings identified proteins that interacted with p-α-syn in the midbrains of TG mice. The requirement for phosphorylation at ser 129 in the interactions of α-syn with VAPB and PTPIP51 was a novel finding. In addition, we found that inhibition of phosphorylation at ser 129 alleviated ER and mitochondrial calcium overload and cell death caused by α-syn overexpression. Phosphorylation of α-syn at ser 129 may therefore affect intracellular calcium regulation via interactions with VAPB and PTPIP51 under pathologic conditions. This finding provides a new way to further elucidate the pathogenesis mediated by p-α-syn.

4. Materials and Methods

4.1. Mice

The Jackson Laboratory (Bar Harbor, ME, USA) provided the WT C57BL mice and the TG mice overexpressing h-syn (017682). The KO mice were bought from Nanjing University's Model Animal Research Center (Nanjing, China). All mice were housed at room temperature (22-25°C) under a 12-2 h light/dark cycle in the Laboratory Animal Center of Capital Medical University (Beijing, China). Animal experiments conformed to the National Institutes of Health (NIH; Bethesda, MD, USA) guidelines for animal care and use. The animal study was reviewed and approved by the Institutional Animal Care and Use Committee. (Capital Medical University Animal Experiments and Experimental Animals Management Committee, AEEI-2020-017).

4.2. Co-Immunoprecipitation (CO-IP)

Brain tissues (2000 μg) or cell extracts (1000 μg) were incubated at 4°C on a rotating platform overnight with anti-h-α-syn, -p-α-syn, or -flag antibody. Magnetic beads (40 μl; Med Chem Express, San Rafael, CA, USA) were rinsed with 500 μl of 150 mM IP buffer, the protein/antibody mixture was then added and incubated at 4°C for 6 h. After washing 3 times, the target antigen-antibody complex was eluted with 20 μl of loading buffer and heated at 95°C for 10 min, followed by silver staining and western blot analysis.

4.3. Silver Staining

Silver staining was performed using a pierce silver Stain Kit (24612; Thermo Scientific, Massachusetts, USA). SDS-PAGE gel was twice-fixed with a mixture of 30% ethanol and 10% glacial acetic acid for 15 min each time. The glue was incubated with 10% ethanol twice for 5 min each time, then with deionized water twice for 5 min each time. A sensitizer working buffer was used to sensitize the glue for 1 min, followed by two quick water rinses. The glue was incubated with stain working solution for 30 min, followed by 2 quick water rinses. The glue was incubated with developer working solution for 2 min until bands appeared. The reaction was terminated with 5% glacial acetic acid.

4.4. Expression and Purification of Recombinant α-syn

Human full-length α-syn cDNA was cloned into the pGEX-4T-1 vector and transformed into BL21 (DE3) *Escherichia coli* (CB105-01; Tiangen, Beijing, China). GST-α-syn expression was induced with 0.1 mM isopropyl-β-D-1-thiogalactopyranoside (IPTG). The purified recombinant GST-α-syn was extracted from the bacterial BL21 lysate using glutathione sepharose™ 4B (GE Health Life Sciences, PA, USA). The α-syn was incubated with human thrombin for 6 h at room temperature. After elution, the buffer was changed into a working buffer (10 μM MgCl2, 20 μM HEPES, and 20 μM of dithiothreitol [pH 7.4]) using a 10 kD molecular weight cut-off filter (Millipore, Bedford, MA, USA). Coomassie brilliant blue staining and western blot were preformed to test the purity of the collected α-syn.

4.5. Preparation of p-α-syn

Preparation of p-α-syn was conducted following previous descriptions [34]. We phosphorylated α-syn at serine 129 using Polo-like kinase 3 (PLK3). 1.2 μL of PLK3 (Thermo Scientific), 50 μL of α-syn, and 0.5μL of ATP (Sigma Aldrich, St. Louis, MO, USA) made up the reaction system. After incubation for 3 h in a water bath at 30°C, the reaction was terminated with 25 mM ethylenediaminetetraacetic acid disodium salt (EDTA-Na2).

4.6. Western Blot

For western blot, the primary antibodies listed below were used: anti-p-α-syn (D1R1R; cell signaling technology, Danvers, MA, USA); anti-h-α-syn (ab138501; Abcam, Cambridge, UK); anti-total-α-syn (pSyn#64; WAKO, Osaka, Japan); anti-β-actin (66009-1-Ig; Proteintech, Chicago, IL, USA); anti-VAPB (1477-1-AP; Proteintech); and anti-PTPIP51 (20641-1-AP; Proteintech). Recombinant proteins, cell, or brain tissue lysates were normalized using BCA protein assay kit (Thermo Scientific). 12% sodium dodecyl sulfate-polyacrylamide gel electrophoresis was used to separate proteins, which were subsequently transferred to PVDF membranes (Millipore). Membranes were blocked with 5% skim milk for 1 h at room temperature, then incubated with primary antibodies overnight at 4°C. The membranes were then thrice-washed with TBST and incubated with fluorophore-conjugated secondary antibodies. After incubation with secondary antibodies for 1 h, the membranes were thrice-washed with TBST and visualized using an Odyssey imaging system (LI- COR Biosciences, Lincoln, NE, USA).

4.7. Immunofluorescence

The primary antibodies listed below were used for immunofluorescence: anti-p-α-syn (Wako, Osaka, Japan); anti-h-α-syn (ab138501; Abcam); anti-TH (ab76442; Abcam); anti-VAPB (1477-1-AP; Proteintech); and anti-PTPIP51 (20641-1-AP; Proteintech). The brain slices were submerged in PBST [0.3% Triton X-100 in 0.01 M PBS] for a duration of 10 min. Subsequently, they were incubated in 5% goat serum (5,424; cell signaling technology) for a period of 60 min. Sections were then subjected to incubation with primary antibodies at a temperature of 4°C for 24 h. Following thrice-wash in PBST, the sections underwent incubation with secondary antibodies for 1 h at room temperature. The next procedure was counterstaining for 15 min with 4',6-diamidino-2-phenylindole (D9542; Sigma-Aldrich, Burlington, MA, USA). Finally, the examination of these sections was conducted utilizing Leica SP8 confocal microscope (Solms, Germany).

4.8. Pre-Embedding Immunogold Electron Microscopy with p-α-syn Antibodies

During deep anesthesia, mice were perfused with a solution of 0.9% NaCl. The residual blood was removed and then followed by perfusion of the circulatory system with a mixture of 4% PFA and 0.075% glutaraldehyde (GA) in 0.1 M PB. Afterward, the brain was extracted and postfixed for 8 h using a solution of 4% PFA and 0.2% GA. The midbrain was then sliced into 50 m-thick slices. These slices were permeabilized for 1 h using PBST, and then incubated for 1 h at room temperature with 5% goat serum (5425, Cell Signaling Technology). Next, the sections were incubated with the C140S antibody at 4°C for 24 h. After thrice-washing with 1% bovine serum albumin (BSA)-PBST, the sections were then incubated with a secondary antibody bound to 1.4 nm gold particles (nanogold-Fab goat anti-mouse IgG [H+L] and nanogold-Fab goat anti-rabbit IgG [H+L], both diluted 1:2500 with 5% BSA-PBST and left at room temperature for 1 h. Following another three washes, the sections were post-fixed with 2% GA. A silver enhancement procedure (2013, Nanoprobes) was performed for 5 minutes, followed by thrice-washing with deionized water. The immunogold-labeled midbrain sections were subsequently re-embedded for ultrathin sectioning. Finally, an ultrathin section analysis was performed using a JEM-2100 electron microscope (JEOL, Tokyo, Japan) to determine the ultrastructural localization of p-α-syn-specific immunolabeling.

4.9. Cell Culture and Transfection

SH-SY5Y cells were grown in DMEM (Gibco, Carlsbad, CA, USA) supplemented with 10% fetal bovine serum (FBS; Gibco). Cells were incubated at 37 °C in 5% CO2; the medium was changed every 3 days. Transfection was performed with plasmids using polyethylenimine (PEI, 23966, linear, MW 25,000; Polysciences, Inc. Warrington, PA, USA,) according to the manufacturer's instructions.

4.10. Primary Neuronal Culture

The Institutional Animal Care and Use Committee of Capital Medical University of Science and Technology granted approval for all experiments conducted in this study. The experiments were executed in accordance with the guidelines outlined in the NIH Guide for the Care and Use of Laboratory Animals. Surgeries were carried out using chloral hydrate anesthesia. Primary neurons were obtained from the brains of mice embryos. The dissociated neurons were grown using neurobasal media (21103-049; Gibco) supplemented with L-glutamine (0.5 mM) and B27 supplement (17504-044; Gibco) on cover slips coated with 0.1 mg/ml poly-L-lysine (P1524; Sigma-Aldrich).

4.11. Measurement of ER and Mitochondrial Calcium

ER calcium measurement was performed using Mag-Fluo4 acetoxymethyl ester (Mag-Fluo4-AM; Molecular Probes) in a cell ER calcium detection assay kit (GMS10267.1 v.A; GENMED, Shanghai, China). Mitochondrial calcium measurement was performed using Mag-

Fluo4 acetoxymethyl ester (Mag-Fluo4-AM; Molecular Probes) in a cell mitochondrial calcium detection assay kit (GMS10153.1 v.A; GENMED). Cellomics high content screening (HCS; Thermo Scientific) was employed to monitor the change in fluorescence at 488/530 nm (green) or 549/595 nm (red).

4.12. Measurement of Mitochondrial Complex I Activity

The manufacturer's instructions were followed for measuring mitochondrial complex I activity using the mitochondrial complex I activity assay kit (AAMT001-1KIT; Merck-Millipore, Darmstadt, Germany). The bicinchoninic acid protein assay kit (23225; Pierce Biotechnology, Rockford, IL, USA) was used to determine the protein content after three cycles of freezing and thawing of cells and tissue. Complex I activity was assessed by measuring the oxidation of nicotinamide adenine dinucleotide (NAD)H to NAD+, which was seen as a reduction in the dye and a corresponding increase in absorbance at 450 nm after 30 min. Cell and tissue lysates were incubated with complex I capture antibody for 3 h at room temperature. Activity is defined as the change in absorbance per minute per amount of material placed in the well, and each sample was evaluated in duplicate.

4.13. JC-1 Staining

We assessed the MMP utilizing the JC-1 probe (T4069; Sigma-Aldrich,). This dual-emission membrane potential-sensitive probe displays a green fluorescent monomer state under low MMP conditions, whereas it aggregates and emits red fluorescence under high MMP conditions. Following three washes with PBS, cells were cultured in 24-well plates and subjected to the addition of JC-1 at 37°C for 30 minutes. Cellomics high content screening (HCS; Thermo Scientific) was employed to monitor the change in fluorescence at 488/530 nm (green) and 549/595 nm (red), ultimately determining the ratio between green and red fluorescence intensity.

4.14. Statistical Analysis

Prism 8.0.1 software (GraphPad, La Jolla, CA, USA) was used for all statistical analyses. The results for each experiment were independently performed at least three times. The data are expressed as the mean ± standard error of the mean (SEM). In all cases, a P value < 0.05 was considered statistically significant.

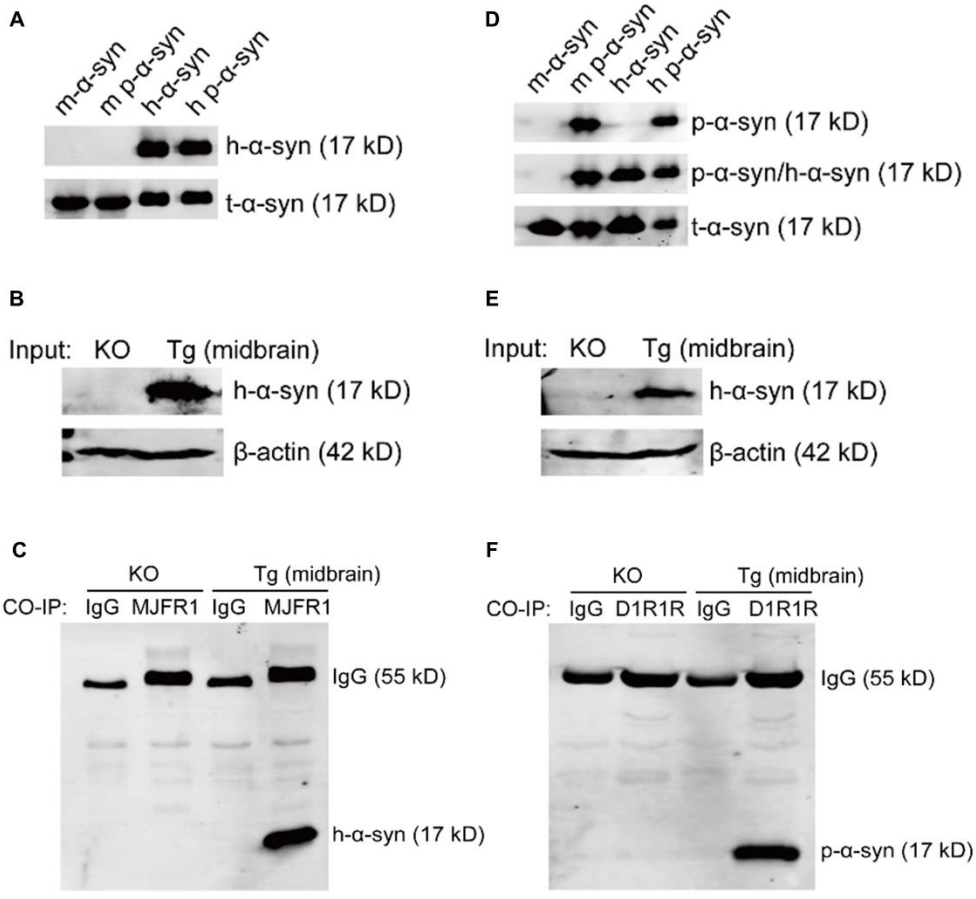

FIGURE S1: Specificity of the h-α-syn and p-α-syn antibodies used in CO-IP/MS experiments. **A)** Recognition of m-α-syn, m p-α-syn, h-α-syn, and h p-α-syn proteins (200 ng) by MJFR1 antibody using western blot. MJFRI antibody specifically recognized human α-syn and p-α-syn proteins. **B)** Western blot was performed to detect h-α-syn in input lysate (input) and **C)** CO-IP proteins in the midbrains of TG mice by MJFR1 antibody. KO mice midbrain tissues served as a negative control group. **D)** The recognition of m-α-syn, m p-α-syn, h-α-syn, and h p-α-syn proteins (200 ng) by D1R1R antibody using western blot. D1R1R antibody specifically recognized p-α-syn proteins. **E)** Western blot was performed to detect p-α-syn in input lysate (input) and **F)** CO-IP proteins in the midbrains of TG mice by D1R1R antibody. KO mice midbrain tissues served as a negative control group.

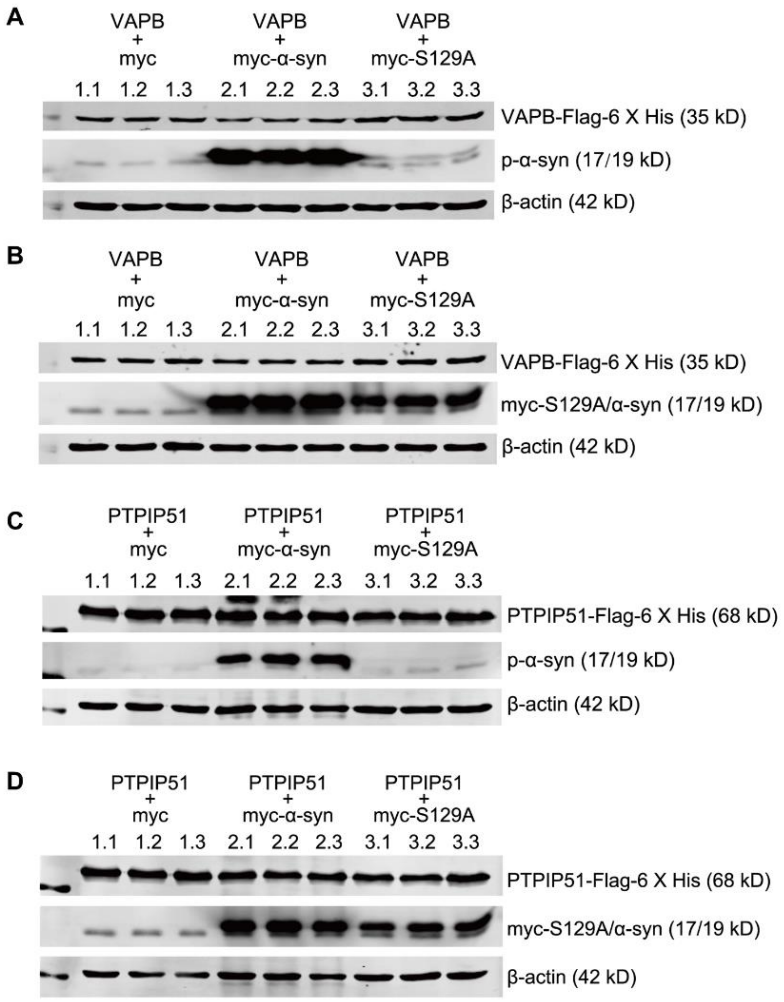

FIGURE S2: The expression of p-α-syn, h-α-syn, VAPB, and PTPIP51 in SH-SY5Y cells. (A, B) SH-SY5Y cells were co-transfected with myc, myc-α-syn, or myc-α-syn S129A and VAPB-Flag-6 X His plasmids. P-α-syn, h-α-syn, and h-α-syn S129A proteins were assessed by western blot by **A)** D1R1R and **B)** MJFR1 antibody. (C, D) SH-SY5Y cells were co-transfected with myc, myc-α-syn, or myc-α-syn S129A and PTPIP51-Flag-6 X His plasmids. P-α-syn, h-α-syn, and h-α-syn S129A proteins were assessed by western blot by **C)** D1R1R and **D)** MJFR1 antibody.

Funding

This work was supported by the National Natural Science Foundation of China (81870994, 82071417, 82301635).

Acknowledgments

This work was supported by the National Natural Science Foundation of China (81870994, 82071417, 82301635).

Author Contributions

W.J.L designed the experiments and collected data. J.J carried out primary neuronal culture and collated data. H.W and T. W contributed to data collection. G.G contributed to the interpretation of the data. J.J drafted the manuscript. H.Y monitored the study progress and edited the manuscript.

Competing Interests

None.

Data Availability

Data will be made available on request.

REFERENCES

[1] Joseph Jankovic, Eng King Tan "Parkinson's disease: etiopathogenesis and treatment." *J Neurol Neurosurg Psychiatry*, vol. 91, no. 8, pp. 795-808, 2020. View at: Publisher Site | PubMed

[2] Samir Kumar Beura, Abhishek Ramachandra Panigrahi, Pooja Yadav, et al. "Role of platelet in Parkinson's disease: Insights into pathophysiology & theranostic solutions." *Ageing Res Rev*, vol. 80, pp. 101681 2022. View at: Publisher Site | PubMed

[3] Hui Ye, Laurie A Robak, Meigen Yu, et al. "Genetics and Pathogenesis of Parkinson's Syndrome." *Annu Rev Pathol*, vol. 18, pp. 95-121, 2023. View at: Publisher Site | PubMed

[4] Hideo Fujiwara, Masato Hasegawa, Naoshi Dohmae, et al. "alpha-Synuclein is phosphorylated in synucleinopathy lesions." *Nat Cell Biol*, vol. 4, no. 2, pp. 160-164, 2002. View at: Publisher Site | PubMed

[5] Latha Devi, Vijayendran Raghavendran, Badanavalu M Prabhu, et al. "Mitochondrial import and accumulation of alpha-synuclein impair complex I in human dopaminergic neuronal cultures and Parkinson disease brain." *J Biol Chem*, vol. 283, no. 14, pp. 9089-9100, 2008. View at: Publisher Site | PubMed

[6] Yue Li, Yi Yuan, Yitong Li, et al. "Inhibition of α-Synuclein Accumulation Improves Neuronal Apoptosis and Delayed Postoperative Cognitive Recovery in Aged Mice." Oxid Med Cell Longev, vol. 2021, pp. 5572899, 2021. View at: Publisher Site | PubMed

[7] Hui Mao, Wei Chen, Linxi Chen, et al. "Potential role of mitochondria-associated endoplasmic reticulum membrane proteins in diseases." *Biochem Pharmacol*, vol. 199, pp. 115011, 2022. View at: Publisher Site | PubMed

[8] Véronik Lachance, Sara-Maude Bélanger, Célia Hay, et al. "Overview of Sigma-1R Subcellular Specific Biological Functions and Role in Neuroprotection." *Int J Mol Sci*, vol. 24, no. 3, pp. 1971, 2023. View at: Publisher Site | PubMed

[9] Gergo Kovacs, Lasse Reimer, Poul Henning Jensen "Endoplasmic Reticulum-Based Calcium Dysfunctions in Synucleinopathies." *Front Neurol*, vol. 12, pp. 742625, 2021. View at: Publisher Site | PubMed

[10] William M Rosencrans, Vicente M Aguilella, Tatiana K Rostovtseva, et al. "α-Synuclein emerges as a potent regulator of VDAC-facilitated calcium transport." *Cell Calcium*, vol. 95, pp. 102355, 2021. View at: Publisher Site | PubMed

[11] Tatiana K Rostovtseva, Sergey M Bezrukov, David P Hoogerheide "Regulation of Mitochondrial Respiration by VDAC Is Enhanced by Membrane-Bound Inhibitors with Disordered Polyanionic C-Terminal Domains." *Int J Mol Sci*, vol. 22, no. 14, pp. 7358, 2021. View at: Publisher Site | PubMed

[12] Xinhe Wang, Katelyn Becker, Nathan Levine, et al. "Pathogenic alpha-synuclein aggregates preferentially bind to mitochondria and affect cellular respiration." *Acta Neuropathol Commun*, vol. 7, no.1, pp. 41, 2019. View at: Publisher Site | PubMed

[13] Melissa J Phillips, Gia K "Voeltz Structure and function of ER membrane contact sites with other organelles." *Nat Rev Mol Cell Biol*, vol. 17, no. 2, pp. 69-82, 2016. View at: Publisher Site | PubMed

[14] Elie Dolgin "How secret conversations inside cells are transforming biology." *Nature*, vol. 567, no. 7747, pp. 162-164, 2019. View at: Publisher Site | PubMed

[15] Celia Kun-Rodrigues, Christos Ganos, Rita Guerreiro, et al. "A systematic screening to identify *de novo* mutations causing sporadic early-onset Parkinson's disease." *Hum Mol Genet*, vol. 24, no. 23, pp. 6711-6720, 2015. View at: Publisher Site | PubMed

[16] Katelyn C Cook, Elene Tsopurashvili, Jason M Needham, et al. "Restructured membrane contacts rewire organelles for human cytomegalovirus infection." *Nat Commun*, vol. 13, no. 1, pp. 4720, 2022. View at: Publisher Site | PubMed

[17] Leonora Szabo, Nadia Cummins, Paolo Paganetti, et al. "ER-mitochondria contacts and cholesterol metabolism are disrupted by disease-associated tau protein." *EMBO Rep*, vol. 24, no. 8, pp. e57499, 2023. View at: Publisher Site | PubMed

[18] Radu Stoica, Kurt J De Vos, Sébastien Paillusson, et al. "ER-mitochondria associations are regulated by the VAPB-PTPIP51 interaction and are disrupted by ALS/FTD-associated TDP-43." *Nat Commun*, vol. 5, pp. 3996, 2014. View at: Publisher Site | PubMed

[19] Patricia Gómez-Suaga, Beatriz G Pérez-Nievas, Elizabeth B Glennon, et al. "The VAPB-PTPIP51 endoplasmic reticulum-mitochondria tethering proteins are present in neuronal synapses and regulate synaptic activity." *Acta Neuropathol Commun*, vol. 7, no. 1, pp. 35, 2019. View at: Publisher Site | PubMed

[20] Sébastien Paillusson, Patricia Gomez-Suaga, Radu Stoica, et al. "α-Synuclein binds to the ER-mitochondria tethering protein VAPB to disrupt Ca(2+) homeostasis and mitochondrial ATP production." *Acta Neuropathol*, vol. 134, no. 1, pp. 129-149, 2017. View at: Publisher Site | PubMed

[21] Huilin Zhang, Jia Liu, Xue Wang, et al. "V63 and N65 of overexpressed α-synuclein are involved in mitochondrial dysfunction." *Brain Res*, vol. 1642, pp. 308-318, 2016. View at: Publisher Site | PubMed

[22] Weijin Liu, Qidi Zhang, Hao Xing, et al. "Characterization of a Novel Monoclonal Antibody for Serine-129 Phosphorylated α-Synuclein: A Potential Application for Clinical and Basic Research." *Front Neurol*, vol. 13, pp. 821792, 2022. View at: Publisher Site | PubMed

[23] Abid Oueslati "Implication of Alpha-Synuclein Phosphorylation at S129 in Synucleinopathies: What Have We Learned in the Last Decade?" *J Parkinsons Dis*, vol. 6, no. 1, pp. 39-51, 2016. View at: Publisher Site | PubMed

[24] Ana Belen Malpartida, Matthew Williamson, Derek P Narendra, et al. "Mitochondrial Dysfunction and Mitophagy in Parkinson's Disease: From Mechanism to Therapy." *Trends Biochem Sci*, vol. 46, no. 4, pp. 329-343, 2021. View at: Publisher Site | PubMed

[25] Mohamed A Eldeeb, Rhalena A Thomas, Mohamed A Ragheb, et al. "Mitochondrial quality control in health and in Parkinson's disease." *Physiol Rev*, vol. 102, no. 4, pp. 1721-1755,2022. View at: Publisher Site | PubMed

[26] Mohamed Bilal Fares, Somanath Jagannath, Hilal A Lashuel "Reverse engineering Lewy bodies: how far have we come and how far can we go?" *Nat Rev Neurosci*, vol. 22, no. 2, pp. 111-131, 2021. View at: Publisher Site | PubMed

[27] Adolfo Garcia Erustes, Manuela D'Eletto, Gabriel Cicolin Guarache, et al. "Overexpression of α-synuclein inhibits mitochondrial Ca(2+) trafficking between the endoplasmic reticulum and mitochondria through MAMs by altering the GRP75-IP3R interaction." *J Neurosci Res*, vol. 99, no. 11, pp. 2932-2947, 2021. View at: Publisher Site | PubMed

[28] Yemima R Butler, Yuqing Liu, Ramhari Kumbhar, et al. "α-Synuclein fibril-specific nanobody reduces prion-like α-synuclein spreading in mice." *Nat Commun*, vol. 13, no. 1, pp. 4060, 2022. View at: Publisher Site | PubMed

[29] Tae-In Kam, Hyejin Park, Shih-Ching Chou, et al. "Amelioration of pathologic α-synuclein-induced Parkinson's disease by irisin." *Proc Natl Acad Sci U S A*, vol. 119, no. 36, pp. e2090132177, 2022. View at: Publisher Site | PubMed

[30] John P Anderson, Donald E Walker, Jason M Goldstein, et al. "Phosphorylation of Ser-129 is the dominant pathological modification of alpha-synuclein in familial and sporadic Lewy body disease." *J Biol*

Chem, vol. 281, no. 40, pp. 29739-29752, 2006. View at: Publisher Site | PubMed

[31] Tim E Moors, Christina A Maat, Daniel Niedieker, et al. "The subcellular arrangement of alpha-synuclein proteoforms in the Parkinson's disease brain as revealed by multicolor STED microscopy." *Acta Neuropathol*, vol. 142, no.3, pp. 423-448, 2021. View at: Publisher Site | PubMed

[32] Melinda A McFarland, Christopher E Ellis, Sanford P Markey, et al. "Proteomics analysis identifies phosphorylation-dependent alpha-synuclein protein interactions." *Mol Cell Proteomics*, vol. 7, no. 11, pp. 2123-2137, 2008. View at: Publisher Site | PubMed

[33] Liliana M Almeida, Brígida R Pinho, Michael R Duchen, et al. "The PERKs of mitochondria protection during stress: insights for PERK modulation in neurodegenerative and metabolic diseases." *Biol Rev Camb Philos Soc*, vol. 97, no. 5, pp. 1737-1748, 2022. View at: Publisher Site | PubMed

[34] Jinxuan Liu, Jinghua Yang "Mitochondria-associated membranes: A hub for neurodegenerative diseases." *Biomed Pharmacother*, vol. 149, pp. 112890, 2022. View at: Publisher Site | PubMed

[35] Andrea Markovinovic, Jenny Greig, Sandra María Martín-Guerrero, et al. "Endoplasmic reticulum-mitochondria signaling in neurons and neurodegenerative diseases." *J Cell Sci*, vol. 135, no. 3, pp. jcs248534, 2022. View at: Publisher Site | PubMed

[36] Stephanie Vrijsen, Céline Vrancx, Mara Del Vecchio, et al. "Inter-organellar Communication in Parkinson's and Alzheimer's Disease: Looking Beyond Endoplasmic Reticulum-Mitochondria Contact Sites." *Front Neurosci*, vol. 16, pp. 900338, 2022. View at: Publisher Site | PubMed

[37] Patricia Gomez-Suaga, Gábor M Mórotz, Andrea Markovinovic, et al. "Disruption of ER-mitochondria tethering and signalling in C9orf72-associated amyotrophic lateral sclerosis and frontotemporal dementia." *Aging Cell*, vol. 21, no. 2, pp. e13549, 2022. View at: Publisher Site | PubMed

[38] György Csordás, David Weaver, György Hajnóczky, et al. "Endoplasmic Reticulum-Mitochondrial Contactology: Structure and Signaling Functions." *Trends Cell Biol*, vol. 28, no. 7, pp. 523-540. View at: Publisher Site | PubMed